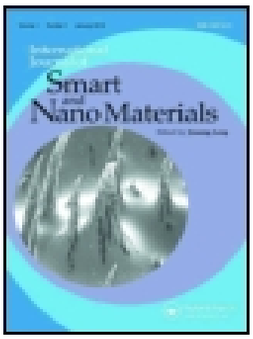

International Journal of Smart and Nano Materials

ISSN: 1947-5411 (Print) 1947-542X (Online) Journal homepage: www.tandfonline.com/journals/tsnm20

Viscoelastic behavior of nanotube-filled polycarbonate: Effect of aspect ratio and interface chemistry

Renée K. Duncan, R. Qiao, J. B. Bult, D. Burris, L. C. Brinson & L. S. Schadler

To cite this article: Renée K. Duncan, R. Qiao, J. B. Bult, D. Burris, L. C. Brinson & L. S. Schadler (2010) Viscoelastic behavior of nanotube-filled polycarbonate: Effect of aspect ratio and interface chemistry, International Journal of Smart and Nano Materials, 1:1, 53-68, DOI: 10.1080/19475411003602732

To link to this article: https://doi.org/10.1080/19475411003602732

International Journal of Smart and Nano Materials
Vol. 1, No. 1, March 2010, 53–68

Taylor & Francis
Taylor & Francis Group

Viscoelastic behavior of nanotube-filled polycarbonate: Effect of aspect ratio and interface chemistry

Renée K. Duncan[a], R. Qiao[b], J.B. Bult[a], D. Burris[c], L.C. Brinson[b] and L.S. Schadler[a]*

[a]*Department of Materials Science and Engineering, Rensselaer Polytechnic Institute, Troy, NY, USA;* [b]*Department of Mechanical Engineering, Northwestern University, Evanston, IL, USA;* [c]*Department of Mechanical Engineering, University of Delaware, Newark, DE, USA*

(*Received 6 January 2010; final version received 6 January 2010*)

A combined experimental and modeling study on the solid-state rheology of multi-walled carbon nanotube (MWNT)/polycarbonate composites as a function, independently, of MWNT aspect ratio and interface chemistry was carried out. Shorter aspect ratio nanotubes lead to greater broadening of the loss modulus peak in frequency space, but there was no effect of aspect ratio on the glass transition temperature. The breadth of the loss modulus peak was found to correlate with the free space parameter, a measure of the spacing between the MWNTs. A new model that accounts for the aspect ratio and distribution in a representative volume element was developed to study these parameters in a controlled setting where morphology was precisely known. Micromechanics modeling was found to correlate well with experimental data. These results shed light on the separate impacts of aspect ratio, dispersion, and interface modification on the solid-state rheology of nanofilled polymers.

Keywords: polymer composite material; nanotube; dynamic mechanical analysis; aspect ratio; rheology

1. Introduction

An understanding of the time-dependent response of multi-walled carbon nanotube (MWNT)-filled polymers is important for predicting their long-term behavior. There have been several excellent studies on the melt rheology of MWNT-filled polymers [1–7] and there is general agreement that increased loading leads to a solid-like response of the composite. The literature, however, reports conflicting results on the impact of dispersion and aspect ratio. For example, it has been shown that better dispersion leads to a solid-like response in the melt at lower loadings [2,8], and it has also been shown that poorer dispersion leads to a more solid-like response [3]. Lower aspect ratio has been shown to increase the solid-like response [4,7] and decrease the viscosity [7]. These discrepancies are, in part, due to the use of surface treatments to change the dispersion. Surface treatment tends to change the aspect ratio, dispersion and the properties and dimensions of the interfacial region surrounding the MWNT simultaneously.

The interfacial region is also important in controlling the time-dependent behavior of MWNT-filled polymers in the solid state. This region can consist of polymer chains immobilized on the surface of nanofillers [9–11], and has been shown to cause mechanical stiffening of the interphase region and thus can be considered as an additional reinforcing

*Corresponding author. Email: schadl@rpi.edu.

ISSN 1947-5411 print/ISSN 1947-542X online

DOI: 10.1080/19475411003602732
http://www.informaworld.com

mechanism in the composite. Experimental evidence of this interphase region can be seen in the polymer sheath that surrounds MWNTs in a polycarbonate composite [7,12] and in the broadening of loss modulus spectra at low frequencies [13,14]. Creep studies [15] have also shown an increase in the relaxation time for shorter relaxation times (as evidenced by lower compliance at short times) and due to an interphase region.

Because of the complex interaction between interphase properties, dispersion, and aspect ratio, it is important to develop models that independently incorporate these parameter and conduct experimental studies to isolate the impacts of each. Fisher and Brinson developed a two-dimensional (2D) model that incorporates micromechanics and interfacial and behavior into a finite element model [16]. Liu and Brinson [17] proposed a hybrid numerical–analytical method for modeling the viscoelastic properties of the polymeric nanocomposites in which the shape of nanoinclusions can be taken into account. Seidel and Lagoudas [18] studied the clustering effect on effective elastic properties of carbon nanotube reinforced composites using a Mori–Tanaka micromechanics approach. The interphase was considered, but spatial information on possible percolation of interphases and local interactions is lost in this micromechanics approach. Liu and Chen [19] calculated the effective mechanical properties of nanotube composites based on a three-dimensional (3D) unit cell containing a single nanotube and considered the reinforcing effect of nanotubes of different aspect ratios, concluding that long nanotubes could provide a stiffer response. However this work considers an idealized case of perfectly aligned nanotubes and cannot incorporate interphase or nanotube interactions. In a different approach, the finite element simulations by Qiao and Brinson [20] develop large representative volume elements with many interacting nanotubes and their associated interphase domains. This work demonstrates that a homogenous interphase zone in a polymer nanocomposite is inadequate to replicate the bulk viscoelastic behavior of polymer nanocomposites and the gradient in the interphase regions must be captured. Because of the ability to model both interphase and nanotube geometry as well as interactions over many nanotubes with varying degrees of dispersion or aspect ratios, the latter approach will be used in the model in this paper.

In this paper, two important points are demonstrated. First, by tailoring the interfacial chemistry, but maintaining the same aspect ratio, or independently varying aspect ratio while maintaining the same interfacial chemistry, the influences of aspect ratio and interfacial response on the composite solid-state rheology can be separated. In addition, through a quantitative analysis of the inter-nanotube spacing, the impact of dispersion on the rheology is revealed. Second, an improved numerical modeling approach is developed that accounts explicitly for the aspect ratio of the nanotubes and their degree of clustering. In the model, these variables can be controlled independently with precision and the modeling results help verify and explain the experimental findings on the effect of aspect ratio and dispersion on behavior.

2. Experimental

2.1. Sample preparation

MWNTs were grown at Rensselaer Polytechnic Institute (RPI) by thermal chemical vapor deposition of xylene–ferrocene feedstock at 700 °C in a quartz tube furnace. Decomposition and deposition of the xylene–ferrocene vapor onto the substrate was allowed to proceed for times of 100, 50 and 20 minutes [21]. The as-received multiwall nanotubes (ARNTs) were grown with a mean diameter of 31 nm (standard deviation of 5 nm) and lengths of 177 μm, 76μm, and 27μm. The 27μm MWNTs were wand sonicated for 30 min in order to create

nanotubes of 3–5 μm in length. Using a method published earlier [22], the untreated nanotubes were chemically modified to create an epoxide-terminated functionalized group, which reacts with the polycarbonate chains to create a covalent linkage. However, subtle changes were made to the processing procedure in order to have the same aspect ratio for both untreated and treated nanotubes in the composites.

As-received nanotubes were put into a tetrahydrofuran (THF) solvent and water bath-sonicated for 6 min. This was done to improve the dispersion of the MWNT bundles, which would allow better infiltration of the surface modification process to individual nanotubes.

MWNT-filled polycarbonate composites were prepared using a precipitation method. Bisphenol A polycarbonate (PC) was dried for 2 h under vacuum at 125°C to remove any residual moisture and then dissolved in THF by water bath sonication for 30 min. In order to obtain the same aspect ratio for the two types of nanotube/matrix composites, the as-received nanotubes underwent the same total sonication time as the functionalized nanotubes. The sonicated MWNT dispersion and PC solution were mixed and stirred with a magnetic stirrer for 3 min. The mixture was poured drop-wise into methanol, which caused the composite to precipitate immediately. The volume ratio of the THF:methanol was 1:5. The composite material was filtered under vacuum and dried under vacuum at 60°C for 15 h. All samples for testing were made by compression molding of 0.3 g of material per sample in a Carver press in a dog bone mold. A temperature of 250°C and pressure of 1 ton for 5 min were the conditions used to produce samples from the gage section of a dog bone mold with dimensions: 8 mm × 4 mm × 1.5 mm (length × width × thickness). The samples were annealed at 200°C for 1 h and slowly cooled to room temperature to remove processing history differences between the samples.

In order to determine the final aspect ratio of the MWNT, a portion of the grip area of the dog bone geometry, approximately 1 mm of both types of composites was dissolved in THF for 48 h. The grip regions of both types of composites were placed on a TEM grid and the aspect ratio of 200 nanotubes were measured. Table 1 shows that the untreated and treated nanotubes had the same aspect ratio for each growth time. Hence, although the sonication step shortened the nanotubes, the surface functionalization procedure used does not cause additional shortening. 0.5 and 2.0 wt % MWNT/polycarbonate composites (of as-received and surface-modified states) were prepared.

2.2. Dynamic mechanical thermal analysis (DMTA)

Samples 4 mm wide, 1 mm thick, and 8 mm long were tested in a Rheometrics Scientific DMTA V in tensile mode as a function of temperature and frequency. For the temperature scans, the temperature was ramped from 25°C to 180°C at a scan rate of 1°C/min. Samples

Table 1. A comparison of the average length and aspect ratio range, showing that the processing procedure used in this study kept the aspect ratio the same for untreated and treated composites.

	As-received MWNT (ARNT)			Modified MWNT (EPNT)		
Initial growth time (min)	Average length (μm)	Average *L*/*d*	*L*/*d* range	Average length (μm)	Average *L*/*d*	*L*/*d* range
100	49.5 ± 13	~1600	1500–1749	48.6 ± 10	~1600	1500–1749
50	12.4 ± 5	~400	300–399	12.0 ± 5	~400	300–399
20 plus 30 (wand sonication)	4.9 ± 2	~150	100–199	4.5 ± 2	~150	100–199

were subjected to a sinusoidal strain amplitude of 0.01% at a constant frequency of 1 Hz and a static force of 50 g. The value of the glass transition temperature was taken as the peak of the loss modulus curve. The frequency scans were done from 0.03 to 200 Hz at five frequencies per decade, in 5°C increments from 120°C to 180°C. At each temperature increment, the sample was held isothermally for 5 min, and then a frequency sweep at the new test temperature conducted. One concern of this study was the reliability of shifting of the curves by the relevant shift factors to produce the master curves. To verify the user-independence of this work, the storage modulus and loss modulus data at different temperatures were analyzed independently at RPI and at Northwestern University. The results were found to be identical. In addition, several samples were run for each condition, and the variation was found to be within the width of the data points reported.

3. 2D model development

As can be seen in the TEM images (Figure 1), multi-walled nanotubes, mostly straight, are well dispersed in the composites for all aspect ratios (L/d) and neither noticeable bundles nor preferred orientation of nanotubes is observed in those images. Thus, it is reasonable to assume that the nanotubes are straight, fully debundled and randomly oriented in the model.

In the representative volume element (RVE), each nanotube is approximated as a straight 1D rod and modeled using beam elements (Figure 2). Since the diameter of beam elements can be separately defined, this approximation enables us to study large aspect ratio nanotubes without requiring large numbers of elements and long computation times. To isolate the aspect ratio effect, uniform diameter and length of nanotubes are enforced in each RVE. In order to reduce the model size and computational time, the aspect ratios are scaled down to 20, 100 and 200 in the models instead of the aspect ratios, $L/d \sim 150$, 400 and 1600 as synthesized in experiments. In this manner, we still accomplish an order of magnitude difference in aspect ratio from which the trends with aspect ratio can be clearly observed.

Considering the material nature of nanotubes, transversely isotropic material properties should be used in the models. Consistent with previous literature [23] five independent elastic constants are required to define the transverse isotropy, which are longitudinal Young's modulus, major Poisson's ratio, longitudinal shear modulus and plane-strain bulk and in-

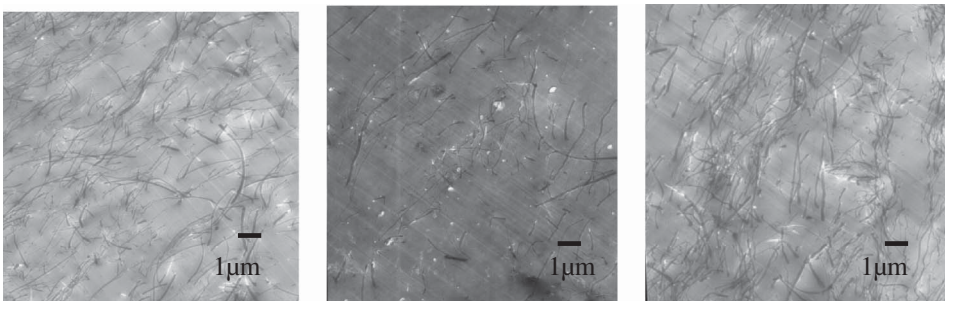

Figure 1. TEM images of 2 wt % untreated MWNT/PC composites: (a) $L/d \sim 150$; (b) $L/d \sim 400$; (c) $L/d \sim 1600$. Note that differences in aspect ratio are not obvious from the TEM slices due to the 50 nm thickness of the slices. All the composites show relatively good dispersion; all images $\times 8000$, 120 kV.

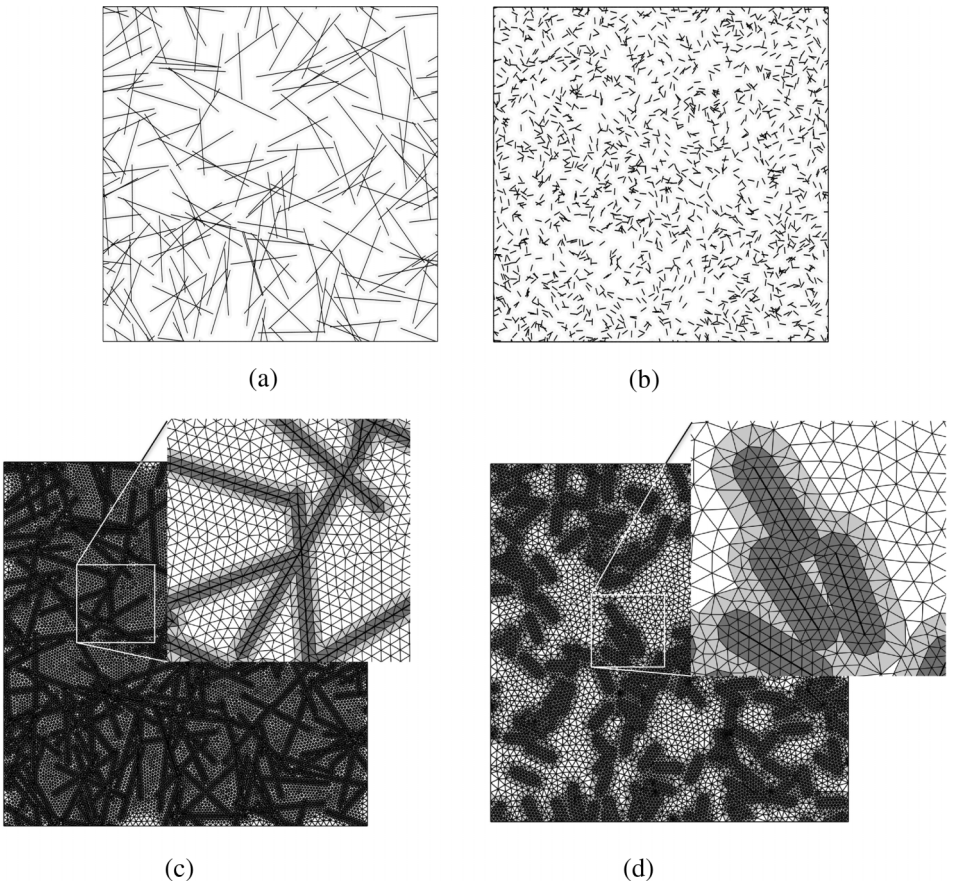

Figure 2. Two RVEs of nanotube composites with same nanotube loading but different aspect ratio, (a) $L/d = 200$ and (b) $L/d = 20$, (c) mesh of RVE with $L/d = 200$, and (d) mesh of RVE with $L/d = 20$, each with inset zoomed in sections showing clearly the double interphase zones surrounding each nanotube.

plane shear moduli, denoted as E_{11}, ν_{12}, G_{12}, K_{23}, and G_{23}, respectively. However, only the longitudinal modulus E_{11} and the major Poisson's ratio ν_{12} were obtained by direct measurements, which are 500 GPa and 0.19, respectively, whereas other elastic constants are still unknown. Since nanotubes were treated as 1D beam elements in the model, the beam section behavior is less important compared to the axial behavior. Therefore, among those five elastic constants, the longitudinal Young's modulus (E_{11}) and longitudinal shear modulus (G_{12}) are most important for the simulation. Herein, for other unknown constants except for G_{12}, we keep the relative ratios between those parameters calculated by Shen and Li [23]: that K_{23} is one order of magnitude lower than E_{11} and G_{23} is three orders lower than E_{11}. For the shear modulus G_{12}, we performed simulations with varying G_{12} values (from one to two orders of magnitude lower than E_{11}) to study the influence on the predicted complex modulus of composites. The results indicate that the G_{12} value has little impact on the simulation. Ultimately, $G_{12} = 1/500E_{11}$ was selected for the longitudinal shear property of the nanotubes.

The interphase regions are modeled as capsules of polymer surrounding the nanotubes (Figure 3) and a thickness five times the nanotube diameter for each layer was used. Our

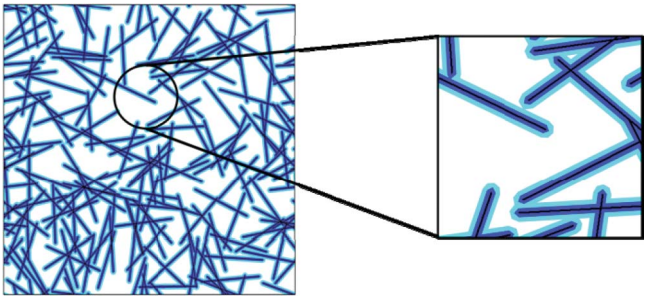

Figure 3. (Color online). Schematic of the model showing the interphase morphology for the random dispersion. Nanotubes are represented as beams in black, whereas the inner-layer interphase is dark blue and outer-layer interphase is light blue (online).

previous work [20] indicates the existence of a gradient in properties of the interphase layer and incorporating this gradient into modeling is critical to reflect the behavior of polymer nanocomposites. Therefore, a two-layer gradient model is used in this simulation to capture the change of interphase properties in the composite. As shown in Figure 3, each nanotube is surrounded by two layers of interphase with equal thickness, the properties of which are assumed to be simply related to those of the matrix based on experimental evidence as described later. Perfect interfacial bonding is assumed so that no contact interaction is considered in this model. The overlapped interphase areas are merged and only counted once in calculations of volume fraction. Finite element simulations are carried out in ABAQUS.

4. Results

4.1. Dispersion

Nanotube dispersion is widely believed to dominate the viscoelastic response of nanoparticle reinforced polymers [2–4,7,24]. Yet, despite this widespread belief, the relationship between dispersion and relevant properties has not been proven for several reasons: the lack of a robust and universal quantitative dispersion/processing technique, the lack of a unified and simple method to quantify dispersion, and because dispersion changes are also often coupled with other important parameter changes (nanoparticle clustering, nanoparticle morphology, etc). In the nanotube-reinforced polymer composites literature, typically one or more representative TEM images are used with qualitative descriptors like poor, good, uniform or random. Here, for each aspect ratio, approximately 10 TEM samples were examined. The average thickness of the TEM samples was approximately 50nm. Figure 1 shows TEM images of 2 wt % MWNT/polycarbonate composites with varying aspect ratio. Using a qualitative assessment as in the majority of papers, these images suggest that the dispersion is relatively “good”.

We also pursued a dispersion quantification method to obtain a characteristic length scale of the particle-free regions of the composites [25]. This basic procedure has the advantage of being simple, universal and physically intuitive. First, an original TEM image is converted into a two-dimensional black/white point map. A Monte Carlo technique is then used to place a statistically large number of squares of prescribed characteristic length in random locations on the surface. The number of particles within each box is counted, and from this single experiment, a histogram of the number of points per square is collected. In this study,

the regions of unfilled polymer are of primary interest since large unfilled or nanotube-free regions escape the influence of this nanoscale filler. As the characteristic square size is reduced towards a critical size, the mode of the distribution tends toward zero. This critical size of one side of the square (where the mode of the distribution first transitions from any positive integer to zero) is the characteristic size of the nanotube-free space and is defined in this study as the free space parameter (FSP). This same methodology is used later to characterize the FSP of the models created to simulate the effect of aspect ratio.

Table 2 shows the FSP for each composite. At 2 wt %, the $L/d \sim 150$ MWNT composites are in closer proximity than in the composites containing MWNT with $L/d \sim 1600$ for both surface treatments. The larger error bar for the EPNT composites suggests greater large scale heterogeneity in those composites. For samples with good dispersion, this result makes sense because the filler loading is the same for the two aspect ratios, thus there are more nanotubes in the $L/d \sim 150$ nancomposite, which, on average, should be closer together. For the 0.5 wt % composites, the FSP is not sensitive to aspect ratio within experimental error. This suggests either a limit to the FSP parameter method, or somewhat poorer dispersion for the shorter aspect ratio MWNT. On the other hand, the surface treatment did improve the dispersion and reduce the FSP at both loadings. It should be noted that because the TEM slices are about 50nm thick, the measured aspect ratio of the nanotubes is different from the real aspect ratio in Table 1. The FSP, however still captures the 2D free space available between the MWNT.

4.2. Temperature sweep studies

Temperature sweeps were used to probe changes in the glass transition temperature. A summary of the glass transition temperature (T_g) for each composite is shown in Table 2. The T_g was taken as the peak of the loss modulus curves (E''). Table 2 shows that the glass transition temperature of both types of composites increases slightly with MWNT loading. For the 0.5 wt % ARNT/PC composites, there is no increase in T_g compared to the neat polycarbonate at all aspect ratios. For the 2.0 wt % ARNT/PC composites, there is an increase of ~2°C for all aspect ratios. Comparing the ARNT and EPNT composites shows that in all cases the EPNT/PC composites have a slightly higher glass transition temperature. The change in glass transition temperature indicates that the surface treatment reduces the mobility of the bulk polymer. This is similar to our earlier results [11,14]. It should be noted that there is no significant change in T_g due to aspect ratio.

Table 2. The free space parameter and glass transition temperature for each composite.

	Average free space parameter (FSP) (μm)		Glass transition temperature (°C)	
Sample	0.5 wt %	2 wt %	0.5 wt %	2 wt %
Neat PC			160.0 ± 2	160.0 ± 2
ARNT				
$L/d \sim 150$	2.26 ± 0.64	0.76 ± 0.16	160.0 ± 1	162.6 ± 1
$L/d \sim 400$	3.10 ± 0.24	1.10 ± 0.21	160.0 ± 1	162.5 ± 2
$L/d \sim 1600$	3.29 ± 1.74	1.30 ± 0.13	160.0 ± 1	162.2 ± 1
EPNT				
$L/d \sim 150$	1.12 ± 0.36	0.3 ± 0.22	161.3 ± 2	163.0 ± 3
$L/d \sim 400$	1.0 ± 0.31	0.5 ± 0.44	162.6 ± 1	163.1 ± 2
$L/d \sim 1600$	1.0 ± 0.29	0.77 ± 0.52	161.9 ± 1	165.1 ± 2

4.3. Master curves

Figure 4 shows the master curves for 2 wt % ARNT- and EPNT-filled polycarbonate composites as compared to neat polycarbonate at different aspect ratios. The incorporation of nanotubes increases the storage modulus of the neat polymer at all frequencies and the effect is even greater for the surface-modified nanotube composites. To highlight any differences in modulus above and below the glass transition temperature, the ratio of the moduli at 10^5 Hz and 10^{-3} Hz was calculated for untreated and EPNT/PC composites (Table 3). As the aspect ratio decreases, the rubbery elastic modulus increases as indicated by an increase in the ratio. In addition, for $L/d \sim 150$ EPNT/PC composites, the ratio is the largest. These results suggest that the surface treatment resulted in a reduction in mobility of the polymer chains as a result of increased interaction between the surface modified nanotubes and the polymer chains. In addition, the larger ratio for the shorter aspect ratio MWNTs indicates that the shorter aspect ratio nanotubes are more effective in reducing mobility and creating a stiffer response in the rubbery domain at low frequency.

The loss modulus results provide further insight into the impact of the interface and the aspect ratio on the rheology. Shifts in the loss modulus curve as reported as changes in T_g in Table 2 indicate that the fillers have impacted the global mobility of the polymer (either via percolation of regions or bulk modification) [20, 31, 32]. Broadening of the loss modulus curves indicates that the relaxation times have been modified locally. The T_g shifts reported in Table 2 and those observed in the loss modulus master curves (e.g. Figure 6) are relatively small and in all cases are accompanied by some degree of broadening. Therefore, in order to highlight any broadening of the loss modulus, the loss modulus was normalized with respect to the neat polymer, as illustrated in Figure 5. On the vertical axis, normalization was achieved by dividing E'' curve values by the maximum value of E'' within the data. The frequency data of the composites were normalized by first dividing all frequencies by the frequency at which the loss modulus peaks and then multiplying these normalized values by the frequency at which the maximum E of neat PC was measured:

$$\omega_{normalized} = \frac{\alpha}{\omega_{peak,composite}} \omega_{peak,PC}.$$

Figure 5 shows that all the composites exhibited broadening compared to the unfilled PC. The broadening is in the low frequency regime indicating immobilization of the polymer chains, or an increase in the number of slow relaxation times. Table 3 shows the full width at half maximum (FWHM) of each of the peaks at 2 wt %. At 0.5 wt %, the ARNT composites show greater broadening on average than the EPNT composites (shown in Figures 5c and 5d). Whereas this might suggest a larger interfacial region in the ARNT composites, recall that the EPNT composites also exhibited a shift. This means that the EPNT had both a local and a global impact on polymer chain mobility. At 2 wt %, the broadening is similar for the two surface treatments and is larger than for the 0.5 wt % composites.

What is perhaps surprising is that the greatest breadth occurs for the shortest aspect ratio at 2 wt % loading. One hypothesis could be that the shorter aspect ratio creates more interfacial region. Using purely geometric reasoning, the increased interfacial region due to the additional nanotube ends, assuming an interface thickness of five times the nanotube diameter, results in 25% more interfacial region. This estimate depends on the size of the interfacial region, for which there are varying size estimates from 10s of nm [14] to 100s of nm [26,27], but in all cases provides one possible mechanism for the increased breadth at low aspect ratios. Figure 6 shows the results of subtracting the unfilled polycarbonate loss

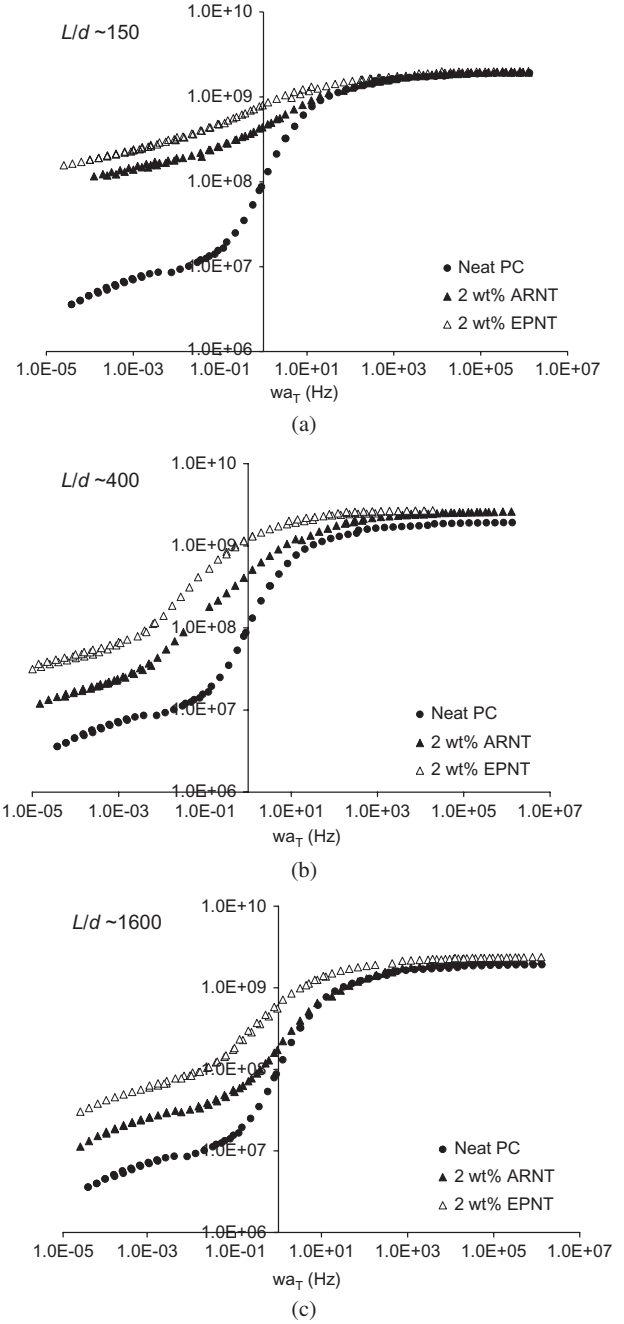

Figure 4. A comparison of the master curves comparison of the storage modulus for pure polycarbonate and constant *L*/*d*, (a) ~150, (b) ~400 and (c) ~ 1600, for treated and untreated nanotube-filled composites.

Table 3. The ratio of storage modulus, E', in the rubbery region to the storage modulus in the glassy region, and the full width half maximum of the loss modulus master curves for 2 wt % treated and untreated samples.

Sample	$\frac{E'@10^{-3}}{E'@10^{5}}$		Full width half maximum of normalized frequency plots	
Neat PC	0.004			
	ARNT/PC	EPNT/PC	ARNT/PC	EPNT/PC
$L/d \sim 150$	0.08	0.13	3.4	3.5
$L/d \sim 400$	0.05	0.02	3.0	2.9
$L/d \sim 1600$	0.01	0.04	2.8	2.8

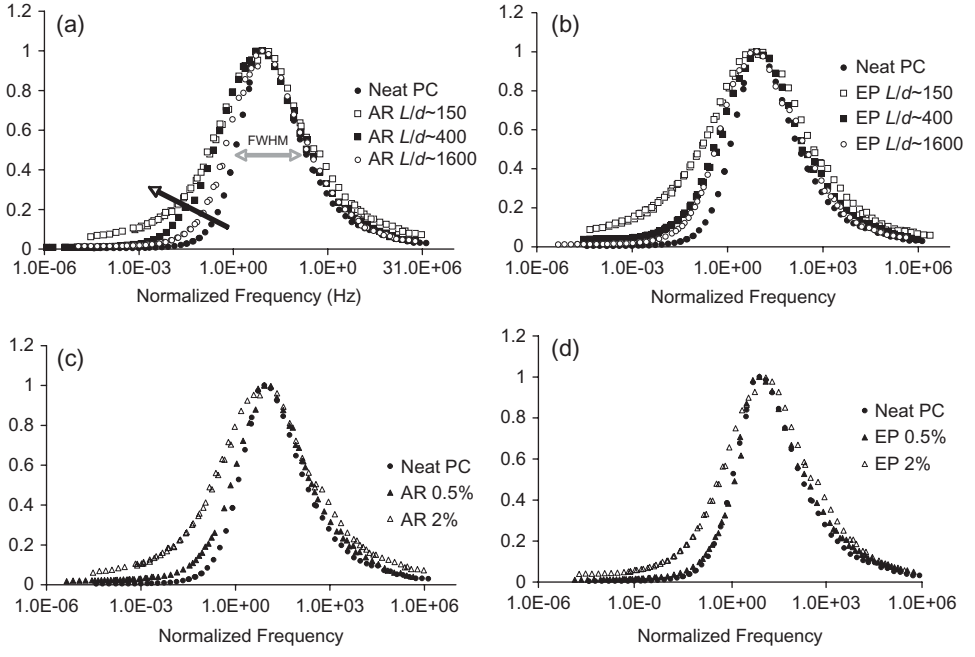

Figure 5. Normalized loss modulus curves comparing the effect of aspect ratio on broadening for (a) as-received nanotube-filled composites and (b) surface-treated nanotube-filled composites at 2 wt %, and the impact of loading at constant $L/d \sim 150$, for (c) untreated and (d) treated nanotube-reinforced composites, showing increased broadening for both composite types.

modulus from the nanocomposite loss modulus. The composites with an aspect ratio of $L/d \sim 150$ have at least 100% greater intensity suggesting that the increased broadening is not simply linearly proportional to the increased interfacial area.

Thus, we hypothesize that the inter-nanotube distance may also play a critical role; similar to the role of inter-particle distance found in nanoparticle filled polymer systems [28–30]. Figure 7 shows a strong correlation between broadening of the loss modulus peak versus free space parameter. This correlation suggests that at a critical inter-nanotube distance, the interfacial regions begin to interact leading to a larger effective interfacial volume and a further reduction in mobility compared to isolated nanotubes of the same concentration and surface chemistry. This effect is related to a percolation of interphase zones throughout the composite [20,31,32], but can exist in non-geometrically percolated systems in two ways. First, in cases

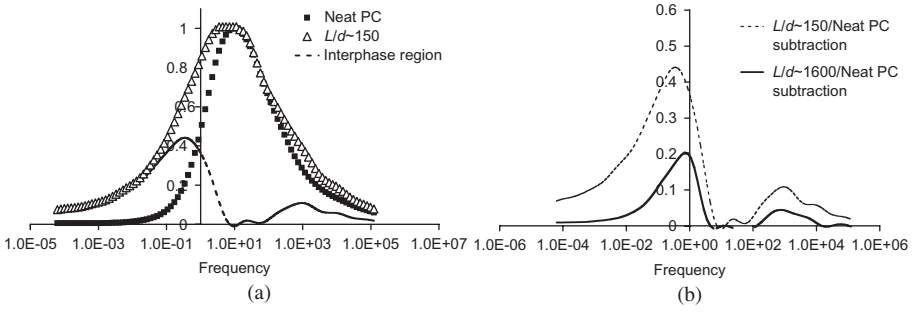

Figure 6. (a) The results of subtracting the pure polymer loss modulus from the 2 wt % untreated composites loss modulus (note frequency axis is not normalized here) highlighting the changes in the loss modulus of the composites compared to that of the neat PC. (b) A comparison of the interphase region loss modulus for aspect ratios of 150 and 1600.

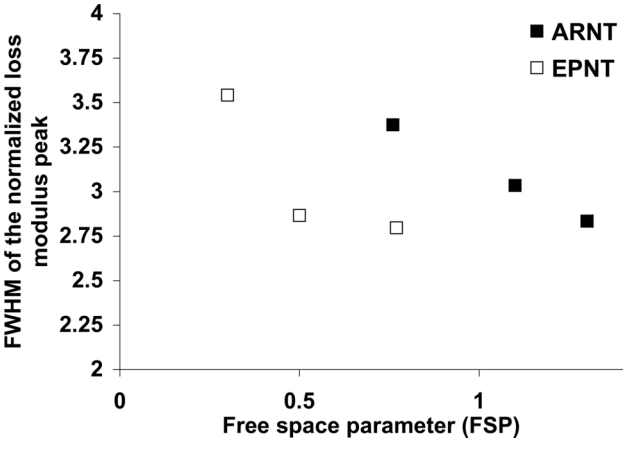

Figure 7. A plot showing the correlation between the FWHM of the normalized loss modulus peak (log scale) and the free space parameter using data from Figure 5.

where the interphase zones are not fully percolated through the composite, there will be regimes of overlapping interphase zones, which are locally percolated, leading to an alteration of bulk response in the form of broadening. Second, as interparticle distances approach a critical value, the properties of the interphase zone can be greatly enhanced over the property changes near isolated particles. This latter mechanism is supported by work on singly and double supported thin films [26,27].

Figure 7 also reveals that for a given FWHM (a given broadness of the loss peak), the ARNT are farther apart than the EPNT in their respective composites. While initially potentially counter-intuitive, this result is likely related to the larger shift of the loss peaks for the EPNT composites, indicating both a global and a local impact on mobility. The global impact is reflected in the shift, decreasing the importance and magnitude of the local impact, the broadening. Consistently, the ARNT composites have more significant local effect on mobility (broadening), and less global impact (shift).

4.4. Modeling results

The aforementioned finite element models of representative volume elements were used to obtain the frequency domain responses of nanocomposites with varying aspect ratio. The dynamic responses of polycarbonate (PC) measured in experiment were used as the material properties of matrix. From Figure 6, we can see that the curves of the subtractions of E'' show major peaks, indicating that the relaxation modes of nanocomposites are different from those for the pure PC and activated with lower frequencies. These modes correspond to a reduced-mobility polymer region, the interphase surrounding the MWNTs. Moreover, the locations for the peaks on the frequency axis are very close for both curves, two decades below the maxima of E'' of neat PC, revealing the independence of relaxation modes of the interphase on the aspect ratio of MWNTs in composites. Based on this observation, we assume that the effective interphase properties are related to those of the bulk polymer matrix by a shift of two decades in the frequency domain. This approximation captures one of the most important characteristics of interphase, that of altered polymer mobility, by introducing the simplest possible assumption on the properties. Considering the two layer gradient interphase in the model, the properties of the inner-layer are determined by shifting PC master curve three decades lower in the frequency domain, while the outer-layer were one decade less mobile so that the average interphase properties were two decades less mobile in comparison with relaxation of neat PC.

The predicted complex moduli of nanocomposites with different aspect ratios were obtained. In order to investigate the impact of the aspect ratio on the breadth of the loss modulus of composites, E'' curves were normalized and shifted using the same method described earlier and the comparison is shown in Figure 8. From this figure, we can see that the E'' curve of the composite with shorter MWNTs, $L/d = 20$, is broader than that of the composite with $L/d = 200$ MWNTs. Although the aspect ratios differ for the computation reasons mentioned earlier, the same trend was observed in the experimental data in Figure 5.

The free space parameters (FSP) measurement was also applied to the microstructures constructed for the FE analysis, using the exact same procedure as the analysis for TEM images of nanocomposites. The FWHM of the normalized E'' of each model versus the FSP are plotted in Figure 9. A strong correlation between the broadness and the free space

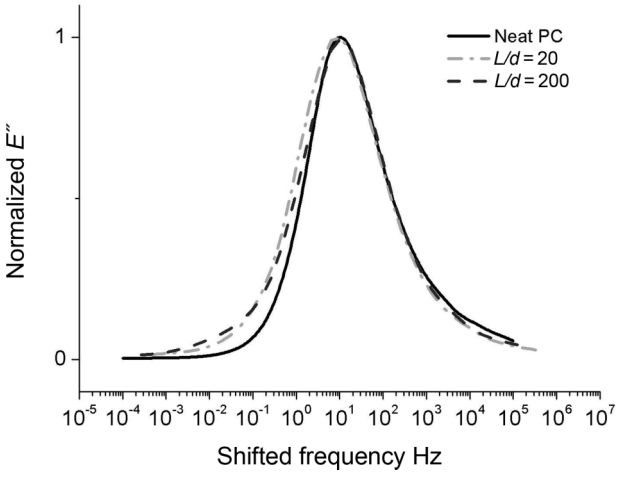

Figure 8. Comparison of normalized loss modulus of composites with different aspect ratios. The frequencies have been shifted to the frequency where the curve of neat PC peaks.

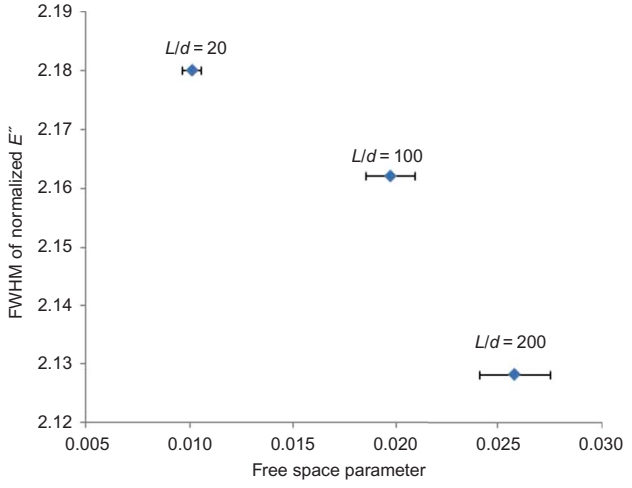

Figure 9. Relationship between free space parameter and broadness (FWHM) of normalized loss moduli calculated from FEM simulations in Figure 8. Error bars arise from several calculations with the Monte Carlo method for the FSP on each geometry.

parameter is shown, which agrees very well with the experimental observation in Figure 7. This result suggests that the free space parameter is able to characterize how the nanotubes affect the overall viscoelastic properties of nanocomposites since less particle-free matrix area implies a larger fraction of polymer chains interacting with the nanoparticles and a correspondingly larger interfacial volume of altered polymer.

However, the magnitudes of FSP and broadness from the numerical simulations differ substantially from those measured in experiments. For the free space parameter, the value obtained experimentally is almost two orders higher than the simulation. This result stems from the 2D nature of the TEM image, only a slice of the nanocomposite, used to calculate the FSP in experiment; in contrast, a 2D model distributed with the same volume fraction of nanotubes is used in the FEM simulation. Thus, the nanotube density apparent in the TEM slice is much lower than that in the model. Moreover, the method to determine FSP highly depends on the image quality because it replies on the color depth to distinguish particles and the matrix. For numerical models, the locations of particles are precisely defined. However, in TEM images, the boundary between nanotubes and bulk polymer is not clear and the threshold used for image binarization can greatly impact on the final calculation of FSP. Thus, while the numerical values of the FSP calculated in models and the FSP obtained experimentally differ, the range observed is similar (about a factor of 4–5 from smallest FSP to largest FSP in both cases) and the qualitative features can be compared well.

Similarly, the broadening of loss modulus predicted in the simulations is also less pronounced compared to the experimental work. This discrepancy could be attributed to the interphase regions and related properties used in the model. Lacking direct measurement of interphase in composites, we assumed all interphase regions surrounding nanotubes have the same thickness of five times the nanotube diameter and further hypothesized the properties of interphase to be related to the properties of bulk polymer by a simple shift in relaxation times. These assumptions capture some basic aspects of the interphase behavior in nanocomposites, but the properties assumed are oversimplified. Additionally, whereas the feature of percolating interphase zones is captured, the additional feature mentioned earlier of

enhanced interphase properties as a function of interparticle distance was not simulated. Thus, more accurate determination of the interphase volume in composites and more sophisticated model for interphase properties are required for a quantitative comparison. Nevertheless, the viscoelastic behavior predicted qualitatively agrees with the experimental observation and helps to confirm the experimental hypotheses.

5. Conclusions

An experimental technique for isolating and quantifying the presence of the volume of interfacial polymer and aspect ratio has been presented. This study found that variance of at aspect ratios that by one order of magnitude have no significant effect on the glass transition temperature, however an epoxide-terminated surface modification process caused an increase in the glass transition temperature by $\sim 3^{\circ}$C. This result indicates that the T_g is influenced by the surface treatment and weight percent of the filler and not by aspect ratio differences. It was also found that the shortest aspect ratio showed a significantly broader loss modulus compared to the longer aspect ratio nanotubes. A broader loss modulus indicates a broader spectrum of relaxation times active in the short aspect ratio composites.

The dispersion of the MWNT/polymer composites was quantified by a free space parameter (FSP). It was observed at 2 wt %, for both composite types, that there was a direct correlation between the broadening of the relaxation modulus and the critical inter-nanotube distance (i.e. FSP). The increased broadening of the normalized loss modulus curves of the $L/d \sim 150$ composites was concluded to be due to the increased size of the interfacial polymer and the smaller free FSP. Simulations were also run on representative unit cells containing nanotubes, interfacial zone and matrix material, predicting the viscoelastic composite properties. Analysis of the predicted loss moduli and FSP confirmed the experimental findings on the relationship between broadness and FSP. This consistency indicates that the FSP is a good parameter to describe the inter-nanotube distance and further predict the broadening of the loss modulus (i.e. presence of interfacial polymer) in nanocomposites. The FSP can be an indicator of when there will be regimes of overlapping interphase zones, which are locally percolated, causing broadening or an indicator of when the interphase zones begin to interact.

The relevance of the findings of this research is three-fold:

- First, the impact of the interfacial polymer was quantified from a bulk testing technique and this behavior was incorporated into analytical models to better predict the macroscopic properties of nanotube-reinforced composites.
- Second, this study was able to correlate the critical inter-nanotube distance and the broadening of the relaxation spectra and hence this correlation can be used to further characterize the interfacial region in models.
- Third, the effect of aspect ratio was isolated from that of the interfacial region. It was found that aspect ratio had no impact on the glass transition temperature and that shorter tubes lead to more broadening (as correlated through the inter-nanotube distance) than longer aspect ratio nanotubes.

Acknowledgments

The authors wish to thank the Nanoscale Science and Engineering Initiative of the National Science Foundation under NSF Award Number DMR-0642573 and CMI0404291. In addition, JB and LSS thank NASA (GSRP grant # NNJ05JG72H), and the Air Force (MURI grant #FA9550-04-1-0367).

References

[1] T. Chatterjee and R. Krishnamoorti, *Dynamic consequences of the fractal network of nanotube-poly(ethylene oxide) nanocomposites*, Phys. Rev. E 75 (2007), 50403.

[2] Y.S. Song, *Effect of surface treatment for carbon nanotubes on morphological and rheological properties of poly(ethylene oxide) nanocomposites*, Polymer Eng. Sci. 46 (2006), pp. 1350–1357.

[3] Y.S. Song and J.R. Youn, *Influence of dispersion states of carbon nanotubes on physical properties of epoxy nanocomposites*, Carbon 43 (2005), pp. 1378–1385.

[4] Y.T. Sung, M.S. Han, K.H. Song, J.W. Jung, H.S. Lee, C.K. Kum, J. Joo, and W.N. Kim, *Rheological and electrical properties of polycarbonate/multi-walled carbon nanotube composites*, Polymer 47 (2006), pp. 4434–4439.

[5] P. Potschke, M. Abdel-Goad, I. Alig, S. Dudkin, and D. Lellinger, *Rheological and dielectrical characterization of melt mixed polycarbonate-multiwalled carbon nanotube composites*, Polymer 45 (2004), pp. 8863–8870.

[6] P. Potschke, A.R. Bhattacharyya, A. Janke, and H. Goering, *Melt mixing of polycarbonate/multi-wall carbon nanotube composites*, Compos. Interface 10 (2003), pp. 389–404.

[7] P. Potschke, T.D. Fornes, and D.R. Paul, *Rheological behavior of multiwalled carbon nanotube/polycarbonate composites*, Polymer 43 (2002), pp. 3247–3255.

[8] Q. Zhang, F. Fang, X. Zhao, Y. Li, M. Zhu, and D. Chen, *Use of dynamic rheological behavior to estimate the dispersion of carbon nanotubes in carbon nanotube/polymer composites*, J. Phys. Chem. B 112 (2008), pp. 12606–12611.

[9] A.-J. Zhu and S.S. Sternstein, *Nonlinear viscoelasticity of nanofilled polymers: Interfaces, chain statistics and properties recovery kinetics*, Compos. Sci. Tech. 63 (2003), pp. 1113–1126.

[10] S.S. Sternstein and A.-J. Zhu, *Reinforcement mechanism of nanofilled polymer melts as elucidated by nonlinear viscoelastic behavior*, Macromolecules 35 (2002), pp. 7262–7273.

[11] A. Eitan, F.T. Fisher, R. Andrews, L.C. Brinson and L.S. Schadler, *Reinforcement mechanisms in MWCNT-filled polycarbonate*, Compos. Sci. Tech. 66 (2006), pp. 1159–1170.

[12] T. McNally, P. Potschke, P. Halley, M. Murphy, D. Martin, S.E.J. Bell, G.P. Brennan, D. Bein, P. Lemoine and J.P. Quinn, *Polyethylene multiwalled carbon nanotube composites*, Polymer 46 (2005), pp. 8222–8232.

[13] M.S.P. Shaffer and A.H. Windle, *Fabrication and characterization of carbon nanotube/poly (vinyl alcohol) composites*, Adv. Mater. 11 (1999), pp. 937–941.

[14] W. Ding, A. Eitan, F.T. Fisher, X. Chen, D.A. Dikin, R. Andrews, L.C. Brinson, L.S. Schadler and R.S. Ruoff, *Direct observation of polymer sheathing in carbon nanotube–polycarbonate composites*, Nano Lett. 3 (2003), pp. 1593–1597.

[15] M. Gan, B.K. Satapathy, M. Thunga, R. Weidisch, P. Tschke and A. Janke, *Temperature dependence of creep behavior of PP–MWNT nanocomposites*, Macromol. Rapid Comm. 28 (2007), pp. 1624–1633.

[16] F.T. Fisher and L.C. Brinson, *Viscoelastic interphases in polymer-matrix composites: Theoretical models and finite-element analysis*, Compos. Sci. Tech. 61 (2001), pp. 731–748.

[17] H. Liu and L.C. Brinson, *A hybrid numerical-analytical method for modeling the viscoelastic properties of polymer nanocomposites*, J. Appl. Mech. Trans. 73ASME (2006), pp. 758–768.

[18] G.D. Seidel and D.C. Lagoudas, *Micromechanical analysis of the effective elastic properties of carbon nanotube reinforced composites*, Mech. Mater. 38 (2006), pp. 884–907.

[19] Y.J. Liu and X.L. Chen, *Evaluations of the effective material properties of carbon nanotube-based composites using a nanoscale representative volume element*, Mech. Mater. 35 (2003), pp. 69–81.

[20] R. Qiao and L.C. Brinson, *Simulation of interphase percolation and gradients in polymer nanocomposites*, Compos. Sci. Tech. 69 (2009), pp. 491–499.

[21] J.B. Bult, W.G. Sawyer, P.M. Ajayan and L.S. Schadler, *Passivation oxide controlled selective carbon nanotube growth on metal substrates*, Nanotechnology 20 (2009), 085302.

[22] A. Eitan, K. Jiang, D. Dukes, R. Andrews and L.S. Schadler, *Surface modification of multiwalled carbon nanotubes: Toward the tailoring of the interface in polymer composites*, Chem. Mater. 15 (2003), pp. 3198–3201.

[23] L.X. Shen and J. Li, *Transversely isotropic elastic properties of multiwalled carbon nanotubes*, Phys. Rev. B 71 (2005), 35412.

[24] F.T. Fisher, A. Eitan, R. Andrews, L.S. Schadler and L.C. Brinson, *Spectral response and effective viscoelastic properties of MWNT-reinforced polycarbonate*, Adv. Compos. Lett. 13 (2004), pp. 105–111.

[25] D.L. Burris, B. Boesl, G.R. Bourne and W.G. Sawyer, *Polymeric nanocomposites for tribological applications*, Macromol. Mater. Eng. 292 (2007), pp. 387–402.
[26] P. Rittigstein, R.D. Priestley, L.J. Broadbelt and J.M. Torkelson, *Model polymer nanocomposites provide an understanding of confinement effects in real nanocomposites*, Nat. Mater. 6 (2007), pp. 278–282.
[27] C.J. Ellison and J.M. Torkelson, *The distribution of glass-transition temperatures in nanoscopically confined glass formers*, Nat. Mater. 2 (2003), pp. 695–700.
[28] A. Bansal, H. Yang, C. Li, K. Cho, B.C. Benicewicz, S.K. Kumar and L.S. Schadler, *Quantitative equivalence between polymer nanocomposites and thin polymer films*, Nat. Mater. 4 (2005), pp. 693–698.
[29] R.D. Priestley, C.J. Ellison, L.J. Broadbelt and J.M. Torkelson, *Materials science: Structural relaxation of polymer glasses at surfaces, interfaces, and in between*, Science 309 (2005), pp. 456–459.
[30] J. Berriot, H. Montes, F. Lequeux, D. Long and P. Sotta, *Evidence for the shift of the glass transition near the particles in silica-filled elastomers*, Macromolecules 35 (2002), pp. 9756–9762.
[31] L.M. Hamming, R. Qiao and P.B. Messersmith and L.C. Brinson, *Effects of dispersion and interfacial modification on the macroscale properties of TiO_2 polymer–matrix nanocomposites*, Compos. Sci. Technol. 69 (2009), pp. 1880–1886.
[32] T. Ramanathan, A.A. Abdala, S. Stankovich, D.A. Dikin, M. Herrera-Alonso, R.D. Piner, D.H. Adamson, J. Liu, R.S. Ruoff, S.T. Nguyen, I. Ihan A. Aksay, R.K. Prud'homme and L.C. Brinson, *Functionalized graphene sheets for polymer nanocomposites*, Nat. Nanotech. 3 (2008), pp. 327–331.